# Three-state antiferromagnetic Potts models: A Monte Carlo study

Jian-Sheng Wang*
*HLRZ, Forschungszentrum Jülich, D-5170 Jülich 1, Federal Republic of Germany*

Robert H. Swendsen
*Department of Physics, Carnegie Mellon University, Pittsburgh, Pennsylvania 15213*

Roman Kotecký
*Department of Mathematical Physics, Charles University, V Holešovičkách 2, 180 00 Praha 8, Czechoslovakia*
(Received 28 March 1990)

We present a study of the three-state antiferromagnetic Potts model in two and three dimensions, using a cluster-flip Monte Carlo simulation algorithm. The new approach enables us to perform simulations with greatly improved efficiency. We have obtained results for the ground-state entropy and critical exponents in two and three dimensions. The low-temperature phase in three dimensions is shown to have long-range order with a finite-size dependence of the magnetization and susceptibility similar to that of the $XY$ model.

## I. INTRODUCTION

In this paper we give a detailed account of our study of the three-state antiferromagnetic Potts model in two and three dimensions, using a cluster-flip algorithm.[1]

Antiferromagnetic Potts models have been shown to possess interesting and unusual properties. The ground-state entropy is nonzero whenever the number of spin states is $q>2$. The $q=3$ model on a square lattice has a critical point only at zero temperature.[2-6] In three dimensions, the evidence indicates the existence of phase transitions for $q=3$, 4, and 5, although the nature of these transitions has been uncertain.[7-12] Notice that the ground-state restrictions are too weak for large $q$ to create an order at low temperatures, and the thermodynamic disorder prevails up to the vanishing temperature. Indeed, using the Dobrushin uniqueness theorem, one can prove[13] that there is no phase transition if $q>3\times 2^d$, where $d$ denotes the dimension of the lattice. Other studies have shown that the addition of second-neighbor interaction,[14-17] mixed anisotropic interactions,[18,19] or an external magnetic field[20] can produce new types of ordering and new phase transitions.

The highly degenerate ground states in the antiferromagnetic Potts models could lead to interesting consequences. Berker and Kadanoff[21] suggested from a one-parameter renormalization-group consideration that, similarly to the $XY$ model in two dimensions, a critical low-temperature phase may appear, with an algebraic decay of correlations. However, this conclusion was criticized, suggesting that it is an artifact of the one-parameter renormalization-group treatment.[20] Banavar, Grest, and Jasnow[7] made the first study of the three-dimensional Potts model for $q=3$ and 4. From a field-theoretic calculation, they conclude that the critical behavior of the three-state model belongs to the universality class of the $XY$ model in three dimensions and the four-state model belongs to the universality class of Heisenberg model, if the transitions are continuous. Their Monte Carlo simulation indicates a continuous transition. They found that there is a nonzero magnetization, also confirmed by Hoppe and Hirst,[8] and recently by Ueno, Sun, and Ono,[12] unlike the behavior suggested by Berker and Kadanoff. On the other hand, Ono[10] suggested that there is no spontaneous magnetization at low temperatures and the low-temperature phase is of the Kosterlitz-Thouless type.[22]

Our Monte Carlo simulation results in two dimensions are consistent with a zero-temperature transition. In three dimensions we find that the critical exponents and low-temperature phase are similar to that of $XY$ model, as proposed in Ref. 7. Our data are much more accurate than previous work[6-8,10,12] due to a new algorithm.[1] In the next section we give a description of our algorithm. Results of simulations for the two- and three-dimensional Potts models are presented in the subsequent sections. We summarize our results in the last section. In the Appendix a careful consideration of order parameters is given.

## II. SIMULATION ALGORITHM

The difficulty encountered in the single-spin-flip algorithm[23,24] is the phenomenon of critical slowing down at a second-order phase transition. The correlation time, which is roughly the time needed to generate a statistically independent configuration, measured in Monte Carlo steps, goes as $\tau\propto L^z$, where $L$ is the linear size of the system and $z$ is dynamic critical exponent ($z\approx 2$ for order-parameter nonconserving dynamics[25-27]). This drastically reduces the accuracy of Monte Carlo data, since the statistical error is inversely proportional to the square root of the number of *independent* configurations. The recently developed cluster-flip-type algorithms[28-33] have

 

been shown to reduce $z$ considerably.[34–36] Thus much better accuracy with less computational efforts can be achieved.

We use[1] a generalization of the algorithm of Swendsen and Wang[28] (SW) to the antiferromagnetic Potts models. This generalization is closely related to Wolff's embedding of Ising reflection variables in $O(n)$ models.[32,37,38] To present the algorithm, let us consider the Potts model defined by the Hamiltonian[39]

$$H=-K\sum_{\langle i,j\rangle}\delta_{\sigma_i,\sigma_j}\ , \tag{1}$$

where the Potts variable $\sigma_i$ takes the value $1,2,\ldots,q$, and the summation is over nearest-neighbor pairs of sites on a square or cubic lattice. $K=J/k_BT$ is a dimensionless coupling constant, and $J<0$ for antiferromagnetic interactions (we set $J/k_B=-1$). The partition function is given by

$$Z=\sum_{\sigma}e^{-H}\ . \tag{2}$$

Following Edwards and Sokal,[30] our algorithm for the Potts antiferromagnetic model may be introduced as a contraction of a joint probability distribution on the spin configurations $\{\sigma_i\}$, $\sigma_i=1,2,3$, and bond configurations $\{n_{ij}\}$, $n_{ij}=0,1,2,3$, where $\langle i,j\rangle$ runs over nearest-neighbor pairs of the lattice sites. Namely, the joint probability

$$\mu_{\text{joint}}=Z^{-1}\prod_{\langle i,j\rangle}\left[(1-p)\delta_{n_{ij},0}+\sum_{\alpha=1}^{3}p\delta_{n_{ij},\alpha}(1-\delta_{\sigma_i,\sigma_j})(1-\delta_{\sigma_i,\alpha})(1-\delta_{\sigma_j,\alpha})\right]\ , \tag{3}$$

where $p=1-e^{-|K|}$. Such a joint-probability distribution yields the following marginal distributions: For configurations $\sigma$ it is just the distribution of the original Potts antiferromagnet; for configurations $n$ it is the distribution with the weights

$$\prod_{n_{ij}=0}(1-p)\prod_{n_{ij}=1,2,3}p2^{N_c}$$

(here $N_c$ is the number of $\alpha$ clusters, defined by the constancy of $n_{ij}=\alpha\neq 0$); different $\alpha$ yield different clusters, and for configurations $\bar{n}$ defined by $\bar{n}_{ij}=0$ if $n_{ij}=0$ and $\bar{n}_{ij}=1$ otherwise, the marginal distribution is defined by the weights

$$\prod_{\bar{n}_{ij}=0}(1-p)\prod_{\bar{n}_{ij}=1}p3^{N_c'}$$

(here the clusters are those just mentioned glued together).

Our algorithm then is actually an alternate application of the following two conditional probabilities:

$$P(n|\sigma)=\begin{cases}\text{surely } n_{ij}=0, \text{ whenever } \sigma_i=\sigma_j\\ n_{ij}=\alpha \text{ with probability } p \text{ and } n_{ij}=0 \text{ with probability } 1-p,\\ \quad\text{whenever } \sigma_i\neq\sigma_j,\ \sigma_i\neq\alpha, \text{ and } \sigma_j\neq\alpha,\end{cases}$$

or, more accurately, the probability $P(n_{A_\alpha}|\sigma,n_{A_\alpha^c})$ under the condition that together with $\sigma$ is fixed a set $A_\alpha$ of bonds on which either $n_{ij}=0$ or $\alpha$ with a fixed configuration on the complement $A_\alpha^c(\langle i,j\rangle\in A_\alpha^c\Longrightarrow n_{ij}\neq 0,\alpha)$,

$$P(n|\sigma)=\begin{cases}\text{surely } n_{ij}=0, \text{ whenever } \sigma_i=\sigma_j\\ n_{ij}=\alpha \text{ with probability } p \text{ and } n_{ij}=0 \text{ with probability } 1-p, \text{ whenever } \sigma_i\neq\sigma_j,\ \sigma_i\neq\alpha, \text{ and } \sigma_j\neq\alpha,\end{cases}$$

for every $\langle i,j\rangle\in A_\alpha^c$, and $P(\sigma|n)$ defined as a random distribution that assigns that distribution to each $\alpha$ cluster with equal probability to those two configurations for which $\sigma_i\neq\sigma_j$, $\sigma_i\neq\alpha$, and $\sigma_j\neq\alpha$.

For actual implementation the algorithm consists of the following steps.

(1) One chooses a pair of Potts states among the $q$ different states at random.

(2) Bonds are formed between nearest-neighbor sites occupied by those chosen states if the two sites are in different Potts states, and a uniformly distributed random number in the interval 0 and 1 is less than $p=1-e^{-|K|}$.

(3) Clusters are identified. A cluster can be either a single site or a set of sites connected through bonds. The sites not in the chosen Potts states are not counted as clusters; their Potts variables do not change.

(4) For each cluster, with equal probability, we either keep its original Potts states, or interchange the chosen Potts state on the sites in the cluster. We then go back to step (1).

For $q=2$, this algorithm reduces to the original SW algorithm for antiferromagnetic Ising models, using the concept of antibonds between spins of opposite signs. The algorithm for $q>2$ updates a subset of the lattice

sites, where the reduced Hamiltonian in one-step updating is that of a dilute antiferromagnet. Of course the reduced (effective) Hamiltonian changes in the next Monte Carlo step, determined by the state of the system. If $q \geq 4$, two or more pairs of states can be updated simultaneously. The relation to Wolff's algorithm[32] is clear, since a $q$-state Potts model can be thought of as an $O(n)$ model with $n = q - 1$ and with unit vectors taking only a discrete sets of values. The reflection of a unit vector with respect to a certain plane is equivalent to the exchange of Potts states.

A key step in implementing this algorithm is a cluster-labeling scheme, so that sites in the same cluster receive the same labeling number, while sites that belong to different clusters have distinct labels. This is done using an auxiliary list of labels. The labeling algorithm is similar to the Hoshen-Kopelman algorithm[40] used in the cluster-counting problem in percolation. An integer array $A(I)$ is initialized to $A(I)=I$, meaning site $I$ has label $I$. If $A(I)<I$, the label of site $I$ is the same as the label of the site $I'=A(I)$. A proper label at any given moment has the property $A(I)=I$. As one goes through each pair of nearest neighbors, if the condition for having a bond in step (2) is fulfilled, the current labels of the two sites are found iteratively: Site $I$ has the label $A(I)$; if the label is equal to $I$, then $I$ is the current label; otherwise site $I$ has the same label as site $A(I)$. One traces back this list until $A(J)=J$; then $J$ is the current label of site $I$. The list is updated so that the labels of the two sites reset to the current, smaller label. A final check is needed to go through the list to ensure that each site has the proper label. The operation needed is proportional to the total number of sites. Thus the computational speed does not slow down as system size increases. The memory requirement is twice the number of sites.

## III. DEFINITION OF ORDER PARAMETER AND SUSCEPTIBILITY

Since the interactions are antiferromagnetic, we expect some kind of staggered order that breaks the sublattice symmetry.[14] We define

$$m_\mu = \frac{2}{L^d}\left[\sum_{i\in a}\delta_{\sigma_i,\mu} - \sum_{i\in b}\delta_{\sigma_i,\mu}\right], \tag{4}$$

where $\mu$ takes values $1,2,\ldots,q$; $L$ is the linear size of the system; $a$ and $b$ are the two sublattices such that the sites on the sublattice $a$ have their nearest neighbors on the sublattice $b$ and the other way around. For the order parameter we may take

$$\langle m \rangle = \frac{1}{q}\sum_{\mu=1}^{q}\langle |m_\mu| \rangle . \tag{5}$$

Our definition is the same as that introduced in Ref. 14 except a constant factor ($\frac{2}{3}$).

The susceptibility is in the disordered phase given by

$$\chi = \frac{L^d}{q}\sum_{\mu=1}^{q}\langle m_\mu^2 \rangle . \tag{6}$$

By noting that each cluster has freedom to choose, independently of other clusters, two possible new states (step 4), we can explicitly perform an average over all possible assignments of the new configurations. Namely, if $N_\alpha^a$ and $N_\alpha^b$ denote the number of sites in the cluster $\alpha$ on the $a$ and $b$ sublattices, respectively, and $N_\alpha = N_\alpha^a + N_\alpha^b$ is the total number of sites in the cluster, assuming that we are interchanging, say, the states 1 and 2, we get

$$m_1 L^d/2 = \sum_\alpha n_\alpha N_\alpha^a - (1-n_\alpha)N_\alpha^b , \tag{7}$$

where $n_\alpha = 1$ if state 1 is on sublattice $a$, and 0 otherwise. Averaging over the random variables $n_\alpha$ for which $\langle n_\alpha \rangle = \frac{1}{2}$ and $\langle n_\alpha n_{\alpha'} \rangle = \frac{1}{4} + \frac{1}{4}\delta_{\alpha,\alpha'}$, we obtain

$$\chi = \frac{L^{-d}}{q}\left[\left\langle \sum_\alpha N_\alpha^2 \right\rangle + \left\langle \left[\sum_\alpha (N_\alpha^a - N_\alpha^b)\right]^2 \right\rangle\right], \quad q=3 . \tag{8}$$

This formula has the advantage over (6) that the variance of $\chi$ is reduced, since it takes into account many configurations.

Another choice of order parameters is given by considering the three Potts states as a unit vector taking three directions 120° apart. Then we have a two-component order parameter. It has been used by Nightingale and Schick,[3] and by Ono.[10] We show in the Appendix that this latter definition is actually more appropriate. We use this definition for the low-temperature susceptibility.

## IV. TWO-DIMENSIONAL RESULTS

### A. Zero-temperature simulation

The efficiency of an algorithm is characterized by a correlation time, determined from the equilibrium time-dependent correlation function, defined by

$$f(t) = \frac{\langle m(t+t_0)m(t_0)\rangle - \langle m(t_0)\rangle^2}{\langle m(t_0)^2\rangle - \langle m(t_0)\rangle^2} , \tag{9}$$

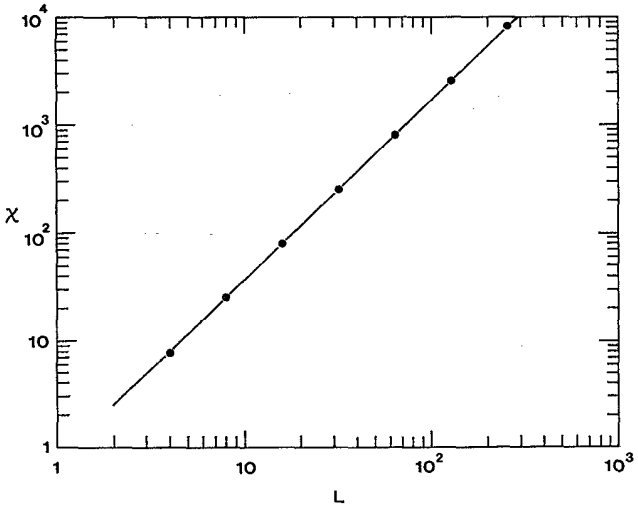


FIG. 1. Log-log plot of the two-dimensional susceptibility $\chi$ vs linear size $L$ at $T=0$. The straight line has a slope $\gamma/\nu = \frac{5}{3}$.

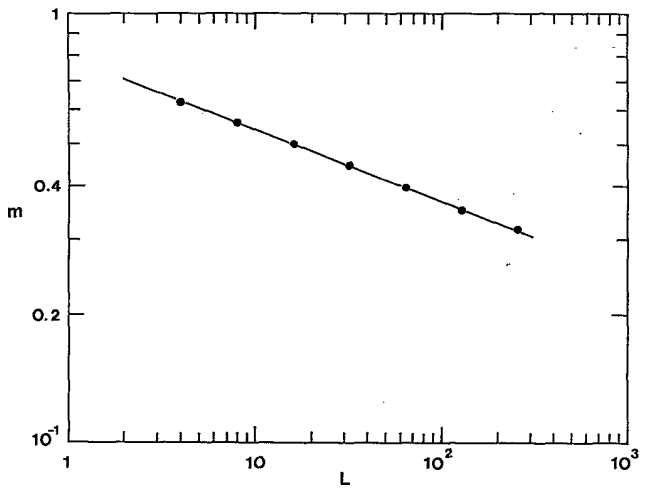


FIG. 2. Log-log plot of the two-dimensional magnetization $m$ vs linear size $L$ at $T=0$. The straight line has a slope $\beta/\nu=\frac{1}{6}$.

where $m$ is the total instantaneous magnetization, defined in Eq. (5), and the angular brackets denote an average over a sequence of configurations generated in a Monte Carlo simulation. The time dependence is, to a very good approximation, exponential, $f(t)\propto e^{-t/\tau}$. The coefficient $\tau$ here is the characteristic correlation time.

For the two-dimensional three-state antiferromagnetic Potts model at zero temperature, the standard Monte Carlo gives a correlation time $\tau_{\text{std}}\simeq 0.32L^z$, with a dynamic critical exponent $z\approx 2.0$. Our algorithm gives a correlation time $\tau\approx 7$ for $L=4$–64. It means that critical slowing down essentially disappears and much more accurate results are obtained.

Figure 1 is a log-log plot of the susceptibility versus size $L$, for $L$ up to 256. A nearly straight line yields a very accurate estimate of the exponents ratio $\gamma/\nu=1.666\pm 0.002$. Assuming scaling, this corresponds to $\eta=2-\gamma/\nu=0.334\pm 0.002$, which characterizes the decay of pair-correlation function, $g(r)\sim r^{-d+2-\eta}$ ($d=2$). Of course, the exponent $\gamma$ or $\nu$ separately is not uniquely defined due to a zero-temperature transition. Park and Widom[41] have recently found an exact value $\gamma/\nu=\frac{5}{3}$, confirming our numerical result.

Figure 2 is a log-log plot for the magnetization. It decreases with size as expected, with the exponents ratio $\beta/\nu=0.170\pm 0.006$ (exact value $\beta/\nu=\frac{1}{6}$). The hyperscaling relation $\gamma/\nu+2\beta/\nu=d$ is satisfied within statistical errors.

### B. Finite-temperature simulation

To calculate the entropy and other thermodynamic quantities, we used the multiple-histogram method.[42] The central idea of the histogram method[43] is to collect distribution of quantities of interest at one temperature; the value at nearby temperatures is generated according to Gibbs formula. The multiple-histogram method[42] combines simulation results at different temperatures, and regenerates data as a function of parameter in the model (typically temperature) in a continuous smooth fashion. As a by-product, the free energy can also be obtained.

In Figure 3 we plotted the magnetization as a function of temperature for different sizes $L=4$, 8, 16, and 32. At high temperatures $m\propto L^{-d/2}$ is observed. At very low temperatures the magnetization decreases with size as $L^{-\beta/\nu}$ as already discussed in Sec. IV A. Our Monte Carlo data are consistent with no spontaneous magnetization at all temperatures in the infinite-size limit. Earlier results (Ref. 14, Fig. 1) might indicate a nonzero magnetization or nonzero $T_c$. This could just be a finite-size effect.

Figure 4 is the reduced free energy per site, defined by $f=L^{-d}\ln Z$, plotted as a function of temperature for sizes $L=4$, 8, and 16. In the high-temperature limit $f$ approaches ln3, while the zero-temperature limit is the ground-state entropy. Finite-size effect shows up at low temperatures.

In two dimensions the ground-state entropy is known to be $s_\infty=\frac{3}{2}\ln\frac{4}{3}$ for an infinite system due to mapping onto an ice model.[44] Finite-size correction is given by[41]

$$s(L)\simeq s_\infty+L^{-2}\ln 2.935\,779\,65\ . \tag{10}$$

We obtained $s(4)=0.5000$, $s(8)=0.4484$, and $s(16)$

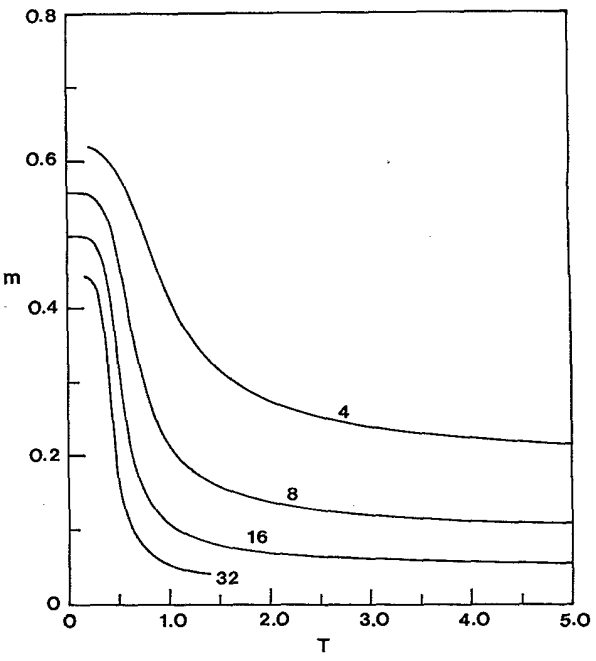


FIG. 3. Magnetization as a function of temperature in two dimensions for size $L=4$, 8, 16, and 32. The smooth curves are obtained using the multiple-histogram method (Ref. 43). This and following plots in two dimensions combine data from five simulations each for $L=4$ and 8, and nine simulations for $L=16$.

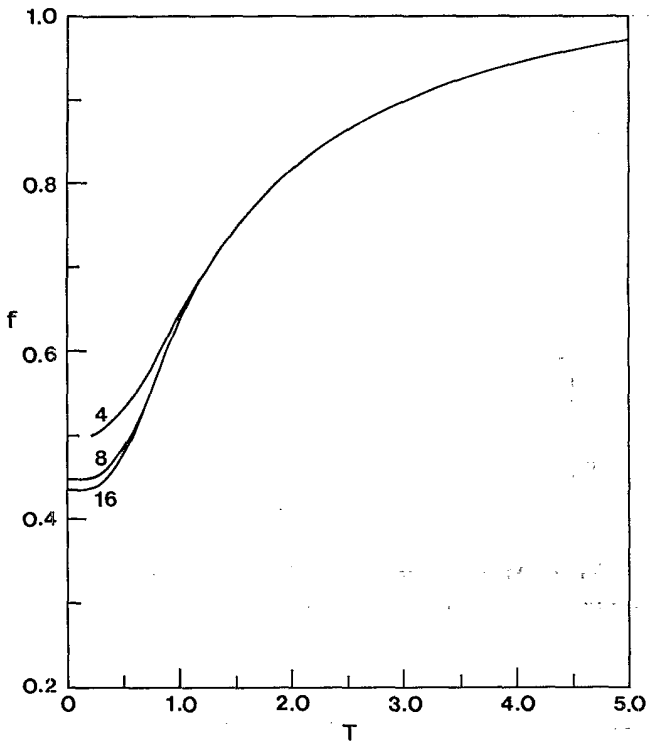


FIG. 4. Reduced free energy $f=L^{-d}\ln Z$ as a function of temperature in two dimensions for size $L=4$, 8, and 16. The value $f$ approaches the ground-state entropy as temperature $T$ approaches zero.

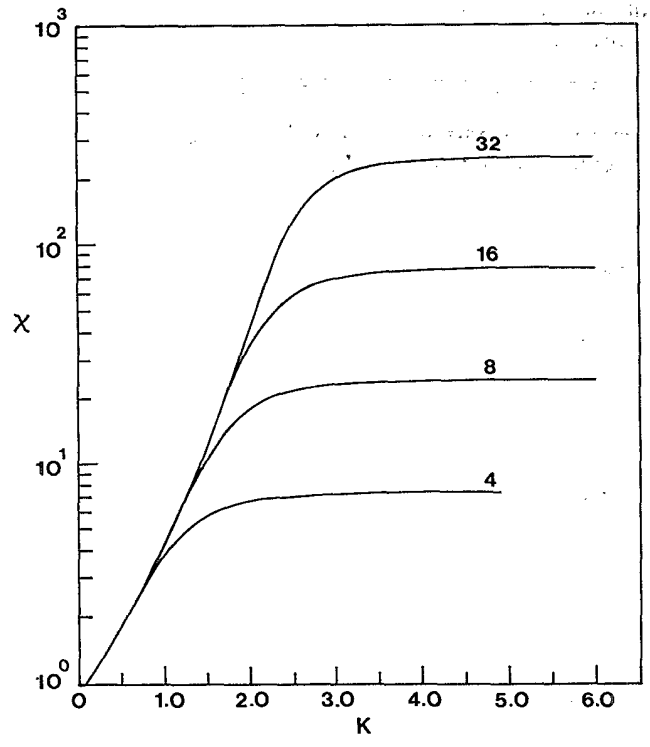


FIG. 5. Susceptibility as a function of coupling strength $K=1/T$ on a semilogarithmic plot for size $L=4$, 8, 16, and 32 in two dimensions.

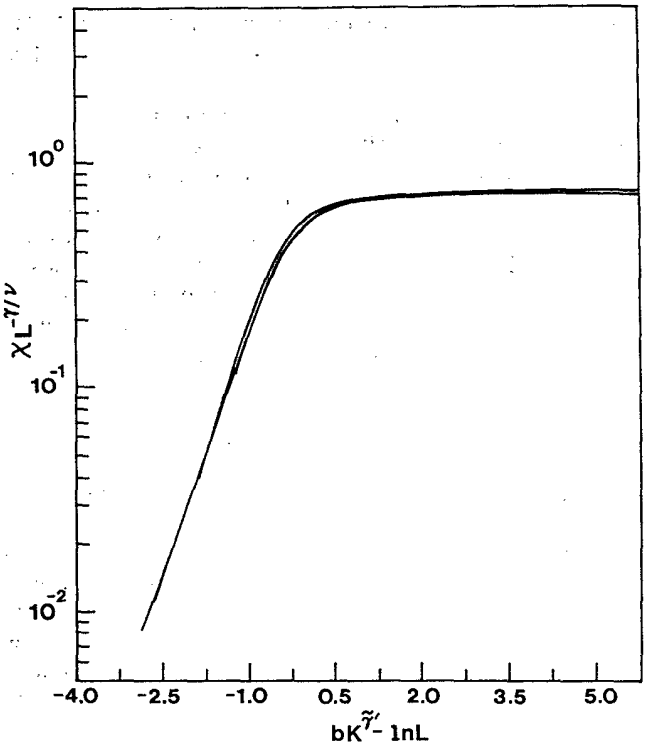


FIG. 6. Scaling plot $L^{-\gamma/\nu}\chi$ vs $\xi/L$ in logarithmic scale, where $\xi=e^{0.90K^{\tilde{\nu}}}$, with $\gamma/\nu=1.666$, $\tilde{\nu}=1.3$, using the same set of data as in Fig. 5.

$=0.4359$ from simulation. These values are in good agreement with exact result in Eq. (10).

In Fig. 5 the susceptibility is plotted against $K=1/T$ on a semilogarithmic scale. A clear curvature is observed, indicating that the susceptibility is growing with $K$ (in the large size limit) faster than a simple exponential. Previous data[6] were analyzed in the form of $\chi\propto|T-T_c|^{-\gamma}$, and it was found $T_c\approx 0$ with $\gamma\approx 5$. Our susceptibility data are not compatible with this functional form.

If we assume a finite-size scaling structure for the susceptibility

$$\chi\simeq L^{\gamma/\nu}\tilde{\chi}(\xi/L)\,, \tag{11}$$

we have to assume that the correlation length takes a form $\xi\simeq e^{bK^{\tilde{\nu}}}$. In the thermodynamic limit the susceptibility then has an essential singularity, $\chi\propto e^{aK^{\tilde{\nu}}}$. Figure 6 is a scaling plot with $\gamma/\nu=1.666$ and $\tilde{\nu}=1.30$. Deviation from scaling is small even for $L=4$. The exponent $\tilde{\nu}$ is in agreement with a phenomenological renormalization-group calculation.[3]

## V. THREE-DIMENSIONAL RESULTS

### A. Correlation time

Correlation time is, for our algorithm, also reduced at the critical temperature in three dimensions. We found that the correlation time is approximately given by

$\tau \approx 2L^{0.48\pm0.04}$ ($L \leq 32$), while for the standard simulation it is found to be $\tau_{\text{std}} \approx \frac{1}{6}L^{2.00\pm0.01}$ ($L \leq 16$). Thus the cluster algorithm becomes advantageous for size $L > 5$.

However, below the critical temperature, where the correlation time is usually size independent, even our algorithm shows a strong size dependence. At a temperature $T/T_c = 0.68$, correlation-time data from system sizes $L = 4$, 8, and 16 are consistent with a dynamic critical exponent $z \approx 2$; it is the same as single-spin-flip dynamics at criticality. This peculiar behavior can be interpreted as that the low-temperature phase exhibits critical fluctuation as suggested by Ono.[10] Our susceptibility data support this interpretation.

### B. Low-temperature behavior

Figure 7 is a plot of magnetization as a function of temperature in three dimensions for system sizes $L = 4$, 8, 16, and 32 (for earlier data, see Ref. 7). Unlike the ferromagnetic Ising models, we found a strong dependence of the order parameter on the size of the system. The magnetization approaches a nonzero value as $1/L$ below $T_c$. Figure 8 is a plot of magnetization as a function of inverse system size, $1/L$, at a temperature $T/T_c = 0.68$. The data linearly extrapolate to a nonzero finite-size limit $m(L = \infty) = 0.491$. Our result is in contrast to Ono's conclusion[10] that magnetization is zero with a massless phase below $T_c$, but is in agreement with that of Banavar *et al.*,[7] Hoppe and Hirst,[8] and Ueno *et al.*[12] As has been observed by Banavar *et al.*,[7] the magnetization at zero temperature, $m(T = 0) = 0.62$, is close to, but less than, $\frac{2}{3}$, the value yielded by maximal possible order. The maximal order (breaking sublattice symmetry) is obtained if one of the spin states is on sublattice $a$ and the other two states are distributed randomly on sublattice $b$.

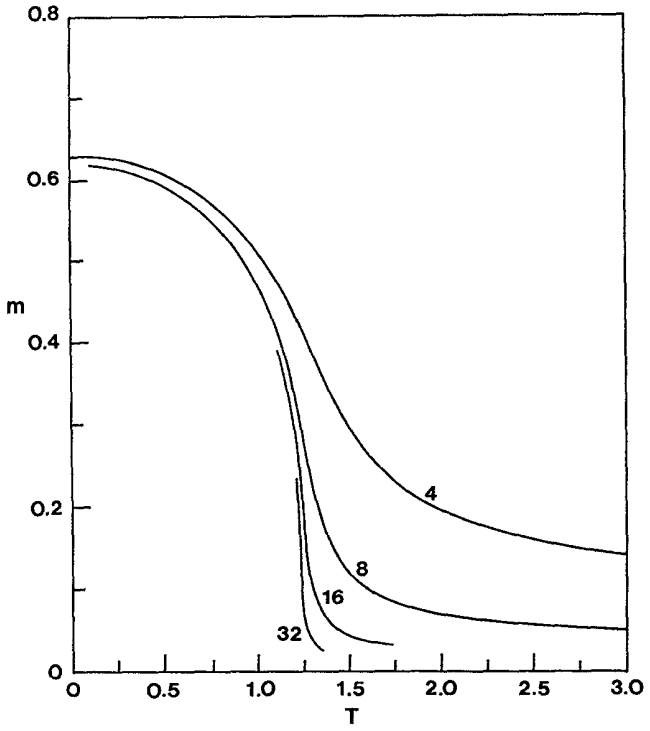


FIG. 7. Magnetization as a function of temperature in three dimensions for system sizes $L = 4$, 8, 16, and 32.

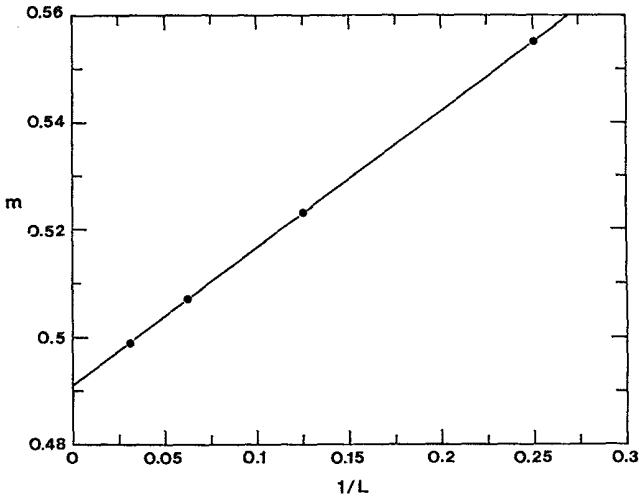


FIG. 8. Magnetization at $T/T_c = 0.68$ vs $1/L$ in three dimensions. The straight line is given by $m = 0.491 + 0.256/L$.

If the (truncated) correlation function decayed algebraically, then the susceptibility, defined by the fluctuation of the magnitude of a two-component vector order parameter,

$$\chi = L^d[\langle \xi_1^2 + \xi_2^2 \rangle - \langle (\xi_1^2 + \xi_2^2)^{1/2} \rangle^2]$$

(see the Appendix for the definition of $\xi_1$ and $\xi_2$), would diverge with system size. Figure 9 is a log-log plot of the

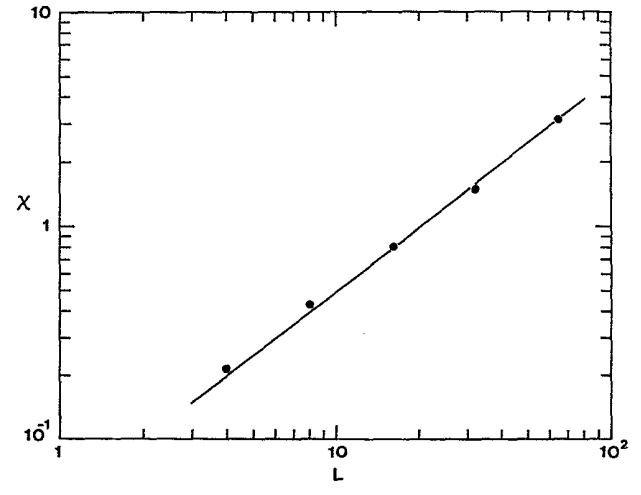


FIG. 9. Susceptibility in three dimensions at $T/T_c = 0.68$ as a function of system size $L$ plotted in log-log scale. The slope of the straight line is 1.

susceptibility at $T/T_c=0.68$ against system size $L$. The susceptibility linearly depends on system size. This behavior is fully consistent with that of the $XY$ model in three dimensions at low temperature. The $1/L$ dependence of the finite-size magnetization is also analogous to the $XY$ model. A spin-wave calculation of the low-temperature magnetization and susceptibility of the $XY$ model would give such a finite-size dependence.[45]

The distribution of the two-component order parameter yields some information about features of the low-temperature phase. At very low temperatures ($T=0.1$, for example), the order parameters take values close to full order. We see sixfold-symmetry peaks for $L=4$ and 8. As system size increases, the peaks become sharper. For $L \geq 16$, only three peaks remain; they are related by exchanging Potts states. The symmetry associated with exchange of sublattices is appearantly broken. As the temperature raises, the peaks becomes less sharp. For temperature not very far from $T_c$, the distribution looks more rotationally symmetric, with a sixfold anisotropy (or threefold for large system size). Very close to $T_c$, the distribution is nearly rotationally symmetric. It appears that the effect in Ono's simulation (Ref. 10, Figs. 5 and 6) is due to a finite observation time. If one simulates time long enough, or the dynamics are fast enough, one would see an approximate circle instead of an arc in the locus of the instantaneous order parameters.

The ground-state entropy is also calculated in three dimensions. Although we have only the values of the residual entropy for $L=4$ and 8 [$s(4)=0.3953$ (10 histogram) and $s(8)=0.3708$ (16 histograms)], we note that they agree with the equation $s(L) \approx s_\infty + L^{-d} \ln 6$, which would predict that $s_\infty = 0.3673$. (Hoppe and Hirst[8] obtained a higher value: 0.376.) This equation is also in reasonable agreement with the exact number of states for an $L=2$ lattice (113.3 versus 126). Borgs and Imbrie[46] rigorously proved that for a class of models with well-defined energetic barriers between phases, the similar coefficient is the logarithm of the number of phases. Even though their theory does not apply in our case, it makes plausible the speculation that ln6 should mean the existence of six phases at low temperatures.

### C. Critical behavior

We used a single histogram method[43] to calculate the specific heat, the susceptibility, and the fourth-order cumulant, simulating at $T=1.225\,49$. The length of the runs were more than $10^6$ Monte Carlo steps except the largest size, $L=64$, which was $1.8\times10^5$ Monte Carlo steps.

The peak of the specific heat grows as the system size increases. Figure 10 is a plot of the peak of specific heat versus size $L$ in a log-log scale. The approach to the asymptotic behavior seems to be rather slow. Assuming that $C_{\text{peak}} \propto L^{\alpha/\nu}$, the effective exponent $\alpha/\nu$ decreases from 0.3 to 0.16, while if one assumes a cusp, $C_{\text{peak}} = C_\infty + aL^{\alpha/\nu}$, the $\alpha/\nu$ value is negative in the range $-0.2 - -0.1$. The data may also be compatible with a logarithmic divergence for $L > 8$. A precise estimate for $\alpha/\nu$ is not possible. This difficulty is also

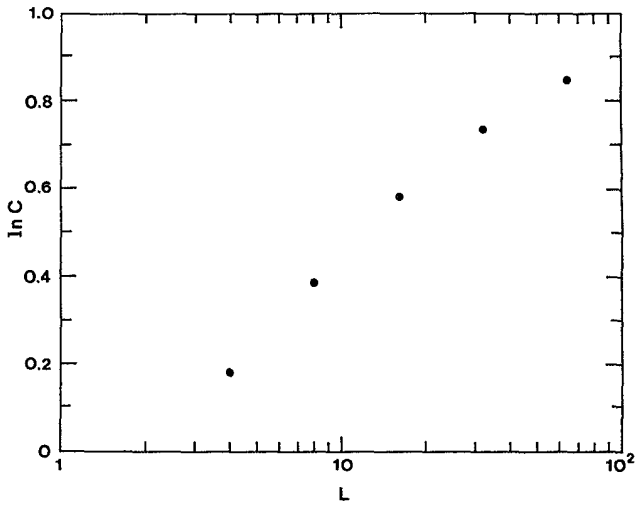


FIG. 10. The peak of specific heat in three dimensions vs size $L$ in log-log scale.

reflected in the location of the peak, shown in Fig. 11. We found that the peak first moves toward lower temperatures as $L$ increases, and then rises back slightly for larger systems. This makes it difficult to apply the standard finite-size scaling for the peak position,

$$T(L) \simeq T_c + bL^{-1/\nu} . \tag{12}$$

A more accurate result is obtained for the critical temperature from the fourth-order cumulant[47]

$$g(T,L) = \frac{1}{2}\left[3 - \frac{\langle m^4 \rangle}{\langle m^2 \rangle^2}\right] \simeq \tilde{g}(|T-T_c|L^{1/\nu}) . \tag{13}$$

In the scaling region close to $T_c$, a different choice of $L$ should have a unique intersection point at $T=T_c$. Figure 12 is $g(T,L)$ for $L=16$, 32, and 64. From this

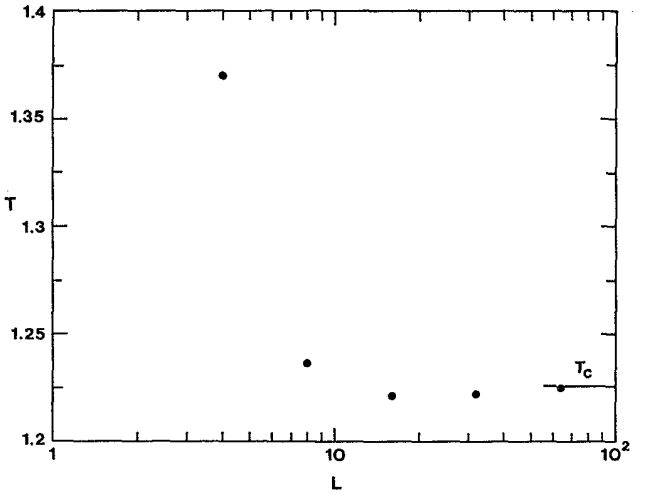


FIG. 11. The location of peak of specific heat in three dimensions as a function of size $L$.

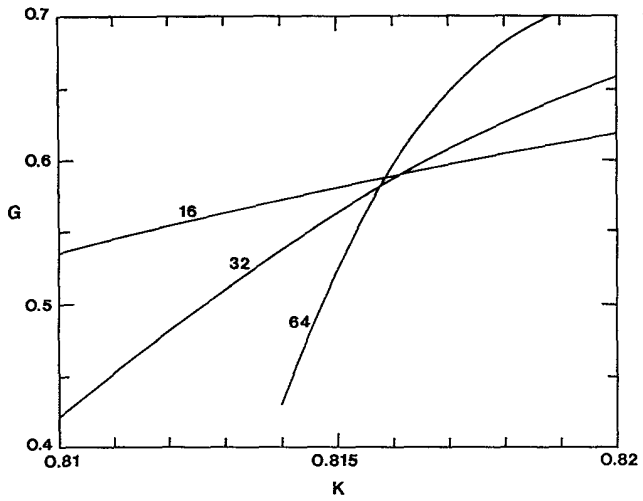


FIG. 12. Fourth-order cumulant $g$ vs inverse temperature $K$ for system size $L=16$, 32, and 64 in three dimensions.

analysis we get an estimate for $T_c=1.2259\pm0.0007$. This should be compared with the results of Ono[10] (1.25), Hoppe and Hirst[8] (1.28±0.04), and Ueno *et al.*[12] (1.235).

The critical exponents $\gamma$ and $\nu$ are obtained from a finite-size scaling plot for the susceptibility, shown in Fig. 13. We find $\gamma/\nu=1.99\pm0.03$ and $\nu=0.66\pm0.03$, using $T_c=1.2259$. These exponents agree with those of the $XY$ model[48–50] within errors. Our results are in disagreement with $\nu=0.58\pm0.01$, $\gamma=1.10\pm0.02$ obtained by Ueno *et al.*, using an interface approach.[12] The discrepancy may be due to the smaller system sizes ($L\leq24$) they have used and the location of the critical temperature.

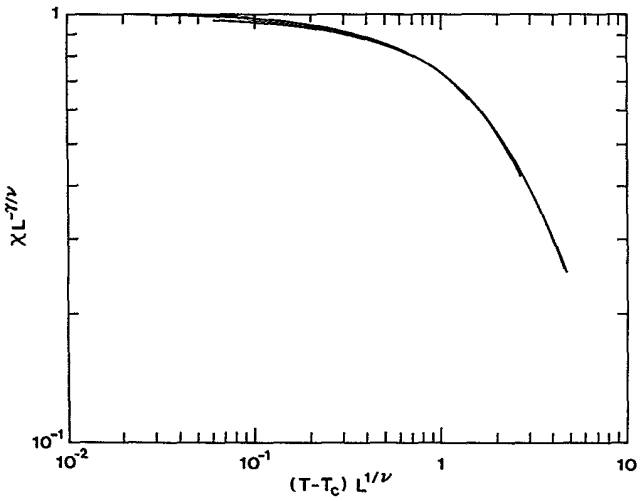


FIG. 13. Scaling plot for the three-dimensional three-state antiferromagnetic Potts model of the susceptibility times $L^{-\gamma/\nu}$ as a function of $(T-T_c)L^{1/\nu}$, using $T_c=1.2259$, $\gamma/\nu=1.99$, and $\nu=0.66$, for $L=8$, 16, 32, and 64.

## VI. CONCLUSION

We have made a high-precision Monte Carlo simulation of the three-state antiferromagnetic Potts model in both two and three dimensions. This is only possible due to a fast algorithm for equilibration. In two dimensions, our results are consistent with previous conclusion that the transition is at zero temperature. The numerical estimates of the exponent $\eta$ and the ground-state entropy are in good agreement with the exact results. The susceptibility is consistent with a form of an essential singularity. In three dimensions, we give estimates of the critical temperature and exponents. The exponents agree with $XY$ model value within statistical errors. At low temperatures, the correlation time, magnetization, and susceptibility data indicate that the correlation length is infinite; but the system has a long-range order (nonzero order parameter). The question remains open whether the anisotropy at low temperatures is relevant to the critical behavior. While Ueno *et al.* claimed a new universality, our results are in favor of $XY$ universality class for the model. Clearly more theoretical understanding is needed to clarify the issue.

## ACKNOWLEDGMENTS

We would like to thank J.L. Lebowitz and the Department of Mathematics of Rutgers University for their generous hospitality while part of this work was being carried out. J.S.W. would like to thank B. Dünweg for a suggestion to consider order parameters in a systematic way that lead to the Appendix. He also thanks K. Binder, H. Müller-Krumbhaar, and W. Selke for stimulating discussions. J.S.W. and R.K. were supported in part by the Rutgers Supercomputer program and by National Science Foundation Grant No. DMR-8612369. R.H.S. was supported by the Rutgers Supercomputing program and by National Science Foundation Grant No. DMR-8613218. Some of the computations were performed at the John von Neumann National Supercomputer Center and at HLRZ, Jülich.

## APPENDIX: ORDER PARAMETERS

Consider three atomic species 1, 2, and 3 (or Potts variables) to be placed on sublattice $a$ and $b$. We shall study order parameters assuming that macroscopic states are completely characterized by particle concentrations $c_1^a,c_2^a,c_3^a$ and $c_1^b,c_2^b,c_3^b$. They are defined by

$$c_\mu^l=\frac{2}{L^d}\left\langle\sum_{i\in l}\delta_{\sigma_i,\mu}\right\rangle , \tag{A1}$$

where $\delta$ is the Kronecker symbol, $\sigma_i$, $\mu=1,2,3$, and $l=a,b$. We use angular brackets to denote a thermodynamic average.

Since each site must be occupied by either 1, 2, or 3, we have a conservation law for the concentration:

$$c_1^a+c_2^a+c_3^a=1 , \tag{A2a}$$

$$c_1^b+c_2^b+c_3^b=1 . \tag{A2b}$$

Thus only four of the six parameters given are independent. Choosing $c_1^a$, $c_2^a$, $c_1^b$, and $c_2^b$ as the independent ones, we may characterize the ferromagnetic order by (suitably rescaled) overall concentrations.

$$\Phi_1=\tfrac{3}{4}(c_1^a+c_1^b)-\tfrac{1}{2}\ , \tag{A3a}$$

$$\Phi_2=\tfrac{3}{4}(c_2^a+c_2^b)-\tfrac{1}{2}\ , \tag{A3b}$$

and the antiferromagnetic order by the difference of sublattice concentrations

$$\Psi_1=c_1^a-c_1^b\ , \tag{A4a}$$

$$\Psi_2=c_2^a-c_2^b\ . \tag{A4b}$$

Now, for a paramagnetic phase we have $\Phi_1=\Phi_2=\Psi_1=\Psi_2=0$, while a complete ferromagnetic order, say $\sigma_i=1$, has $\Phi_1=1$, $\Phi_2=-\frac{1}{2}$, $\Psi_1=0$, $\Psi_2=0$, and a complete antiferromagnetic order, say with 1 and 2 on sublattice $a$ and $b$, respectively, has $\Psi_1=1$, $\Psi_2=-1$, $\Phi_1=\frac{1}{4}$, $\Phi_2=\frac{1}{4}$.

The dependent variables $\Phi_3$, $\Psi_3$ can be defined in a similar fashion with the conservation law Eq. (A2) rewritten as

$$\Phi_1+\Phi_2+\Phi_3=0\ , \tag{A5a}$$

$$\Psi_1+\Psi_2+\Psi_3=0\ . \tag{A5b}$$

Let us consider invariants of the symmetries of the model (needed, e.g., when constructing a Landau Hamiltonian). Taking into account the symmetries with respect to arbitrary permutations of atomic species 1,2,3 and with respect to the interchange of the sublattices $a$ and $b$, we infer that invariants are symmetric functions in the variables $\Phi_1$, $\Phi_2$, $\Phi_3$ as well as $\Psi_1$, $\Psi_2$, $\Psi_3$, and are symmetric with respect to the transformation $\Psi\rightarrow-\Psi$. The second-order invariants are

$$\Phi_1^2+\Phi_2^2+\Phi_3^2\ , \tag{A6a}$$

$$\Psi_1^2+\Psi_2^2+\Psi_3^2\ . \tag{A6b}$$

The third-order term

$$\Phi_1^3+\Phi_2^3+\Phi_3^3 \tag{A7}$$

contains only ferromagnetic order parameters and, in the Landau Hamiltonian, may be viewed as that one responsible for a first-order phase transition in the ferromagnetic Potts model in three and higher dimensions. The fourth-order terms are

$$(\Phi_1^2+\Phi_2^2+\Phi_3^2)^2\ , \tag{A8a}$$

$$(\Psi_1^2+\Psi_2^2+\Psi_3^2)^2\ . \tag{A8b}$$

These are the only possible invariants up to the fourth order.

Let us choose independent parameters (cf. Ref. 18) that diagonalize the quadratic invariant, say $\Phi_1-\Phi_2$, $\Phi_3$, $\Psi_1-\Psi_2$, and $\Psi_3$. Rescaling (with respect to shifting) them slightly we get the Landau Hamiltonian

$$H_\xi=a+b(\xi_1^2+\xi_2^2)+c(\xi_1^2+\xi_2^2)^2\ , \tag{A9}$$

$$H_\eta=d+e(\eta_1^2+\eta_2^2)+f\eta_1\left[\frac{\eta_1^2}{3}-\eta_2^2\right]+g(\eta_1^2+\eta_2^2)^2\ , \tag{A10}$$

with order parameters

$$\xi_1=-\frac{\sqrt{3}}{2}(c_3^a-c_3^b)\ , \tag{A11a}$$

$$\xi_2=\tfrac{1}{2}[(c_1^a-c_1^b)-(c_2^a-c_2^b)]\ , \tag{A11b}$$

and

$$\eta_1=-\tfrac{3}{4}(c_3^a+c_3^b)+\tfrac{1}{2}\ , \tag{A12a}$$

$$\eta_2=\frac{\sqrt{3}}{4}[(c_1^a+c_1^b)-(c_2^a+c_2^b)]\ . \tag{A12b}$$

These are the order parameters used by Ono[10] and have an illustrative interpretation when Potts spins $\sigma_i$ are viewed as unit vectors in three directions forming the angles $2\pi/3$. Taking into account that the concentrations $c_\mu^l$ belong to the interval [0,1], the vector $\xi=(\xi_1,\xi_2)$ is restricted to fall within a uniform hexagon of diameter 1, while $\eta=(\eta_1,\eta_2)$ falls into a uniform triangle (cf. Ref. 10). In term of order parameters $\xi$ and $\eta$, the three possible states of perfect ferromagnetic order are described by unit vectors $\eta$ in the vertices of the triangle, while $\xi=0$. The states of perfect antiferromagnetic order are represented by unit vectors $\xi$ in the vertices of the hexagon with vector $\eta$ (of the length $\frac{1}{2}$) in the centers of the sides of the triangle. For the three-state Potts antiferromagnet in three dimensions a broken-sublattice (BS) order is expected to occur at low temperatures. Namely, the order with one sublattice is occupied by one of the three states, while the other sublattice is occupied by the remaining two states at random. The BS states are represented by vectors $\xi$ of the length $\sqrt{3}/2$ in the centers of the sides of the hexagon with vector $\eta$ of the length $\frac{1}{4}$ in the vertices of a suitably rescaled triangle.

The state constructed under periodic boundary conditions has all the symmetries of the model. In particular, all the concentrations $c_\mu^l$ are clearly equal to $\frac{1}{3}$ and the parameters $\Phi$ and $\Psi$ are, strictly speaking, vanishing. In Sec. III we are using (following Ref. 7) the order parameter $\langle m\rangle$ defined by formulas (4) and (5). This parameter may be thought of as a sum of the parameter $|\Psi_1|+|\Psi_2|+|\Psi_3|$ over all ordered states (existing at given temperatures). Notice, however, that it cannot discern antiferromagnetic and BS states.

*Present address: Institut für Physik, Johannes-Gutenberg Universität, Staudinger Weg 7, D-6500 Mainz, Federal Republic of Germany.

[1]J.-S. Wang, R. H. Swendsen, and R. Kotecký, Phys. Rev. Lett. **63**, 109 (1989).
[2]R. Baxter, Proc. R. Soc. London, Ser. A **383**, 43 (1982).
[3]M. P. Nightingale and M. Schick, J. Phys. A **15**, L39 (1982).
[4]C. Jayaprakash and J. Tobochnik, Phys. Rev. B **25**, 4890

(1982).
[5]T. Temesvari, J. Phys. A **15**, L625 (1982).
[6]F. Fucito, J. Phys. A **16**, L541 (1983).
[7]J. R. Banavar, G. S. Grest, and D. Jasnow, Phys. Rev. Lett. **45**, 1424 (1980); Phys. Rev. B **25**, 4639 (1982).
[8]B. Hoppe and L. L. Hirst, J. Phys. A **18**, 3375 (1985); Phys. Rev. B **34**, 6589 (1986).
[9]R. Kotecký, Phys. Rev. B **31**, 3088 (1985).
[10]I. Ono, Prog. Theor. Phys. Suppl. **87**, 102 (1986).
[11]M. C. Marques, J. Phys. A **21**, 1061 (1988); **21**, 1297 (1988).
[12]Y. Ueno, G. Sun, and I. Ono, J. Phys. Soc. Jpn. **58**, 1162 (1989).
[13]H.-O. Georgii, *Gibbs Measures and Phase Transitions* (de Gruyter, Berlin, 1988), p. 148.
[14]G. S. Grest and J. R. Banavar, Phys. Rev. Lett. **46**, 1458 (1981).
[15]M. P. M. den Nijs, M. P. Nightingale, and M. Schick, Phys. Rev. B **26**, 2490 (1982).
[16]J. R. Banavar and F. Y. Wu, Phys. Rev. B **25**, 1511 (1984).
[17]I. Ono, J. Phys. Soc. Jpn. **53**, 4102 (1984).
[18]W. Kinzel, W. Selke, and F. Y. Wu, J. Phys. A **14**, L399 (1981).
[19]K. Yasumura, J. Phys. A **20**, 4975 (1987).
[20]Z. Racz and T. Vicsek, Phys. Rev. B **27**, 2992 (1983).
[21]A. N. Berker and L. Kadanoff, J. Phys. A **13**, L259 (1980).
[22]J. M. Kosterlitz and K. J. Thouless, J. Phys. C **6**, 1181 (1973).
[23]N. Metropolis, A. W. Rosenbluth, M. N. Rosenbluth, A. H. Teller, and E. Teller, J. Chem. Phys. **21**, 1087 (1953).
[24]K. Binder, *Monte Carlo Methods in Statistical Physics,* edited by K. Binder (Springer-Verlag, Berlin, 1979); *Applications of the Monte Carlo Method in Statistical Physics,* edited by K. Binder (Springer-Verlag, Berlin, 1984).
[25]P. C. Hohenberg and B. I. Halperin, Rev. Mod. Phys. **49**, 435 (1977).
[26]S. K. Ma, *Modern Theory of Critical Phenomena* (Benjamin, Reading, MA, 1976), Chaps. 11–14.
[27]S. Wansleben and D. P. Laudau, J. Appl. Phys. **61**, 3968 (1987).
[28]R. H. Swendsen and J.-S. Wang, Phys. Rev. Lett. **58**, 86 (1987).
[29]D. Kandel, E. Domany, D. Ron, A. Brandt, and E. Loh, Jr., Phys. Rev. Lett. **60**, 1591 (1988); D. Kandel, E. Domany, and A. Brandt, Phys. Rev. B **40**, 330 (1988).
[30]R. G. Edwards and A. D. Sokal, Phys. Rev. D **38**, 2009 (1988).
[31]F. Niedermayer, Phys. Rev. Lett. **61**, 2026 (1988).
[32]U. Wolff, Phys. Rev. Lett. **62**, 361 (1989).
[33]R. C. Brower and P. Tamayo, Phys. Rev. Lett. **62**, 1087 (1989).
[34]D. W. Heermann and A. N. Burkitt, Physica A **162**, 210 (1990); J.-S. Wang, *ibid.* **164**, 240 (1990).
[35]P. Tamayo, R. C. Brower, and W. Klein, J. Stat. Phys. **58**, 1083 (1990).
[36]U. Wolff, Phys. Lett. B **228**, 379 (1989).
[37]R. G. Edwards and A. D. Sokal, Phys. Rev. D **40**, 1374 (1989).
[38]M. Hasenbusch, Nucl. Phys. **B333**, 581 (1990).
[39]R. B. Potts, Proc. Cambridge Philos. Soc. **48**, 106 (1962).
[40]J. Hoshen and R. Kopelman, Phys. Rev. B **14**, 3438 (1976).
[41]H. Park and M. Widom, Phys. Rev. Lett. **63**, 1193 (1989).
[42]A. M. Ferrenberg and R. H. Swendsen, Phys. Rev. Lett. **63**, 1195 (1989); Computers in Physics **3(5)**, 101 (1989); see also P. B. Bowen *et al.*, Phys. Rev. B **40**, 7439 (1989).
[43]A. M. Ferrenberg and R. H. Swendsen, Phys. Rev. Lett. **61**, 2635 (1988).
[44]E. Lieb, Phys. Rev. **162**, 162 (1967).
[45]K. Kawasaki and H. Mori, Prog. Theor. Phys. (Kyoto) **27**, 529 (1962); **28**, 690 (1962).
[46]C. Borgs and J. Imbrie, Commun. Math. Phys. **123**, 305 (1989).
[47]K. Binder, Z. Phys. B **43**, 119 (1981).
[48]M. Ferer, M. A. Moore, and M. Wortis, Phys. Rev. B **8**, 5205 (1973).
[49]J. C. Le Guillon and J. Zinn-Justin, Phys. Rev. Lett. **39**, 95 (1977).
[50]D. Z. Albert, Phys. Rev. B **25**, 4810 (1982).